UNIVERSITY OF READING

Department of Mathematics

Computer Simulations of Dipolar Fluids Using Ewald Summations

Naomi J. K. Withey

August 2012

This is a dissertation submitted in partial ful lment of the requirement for the degree of Master of Science.

Abstract

The Ewald summation method is a key way to improve the accuracy of computer simulations, which are essential in building our understanding of the behaviour of dipolar substances, particularly magnetic fluids. Implementation and accuracy in a three dimensional periodic geometry are discussed comprehensively, drawing together many of the key publications in this field. The procedure is then extended to account for the confined geometry representative of thin layers of ferrofluids. This is done using the EW3DLC

Contents

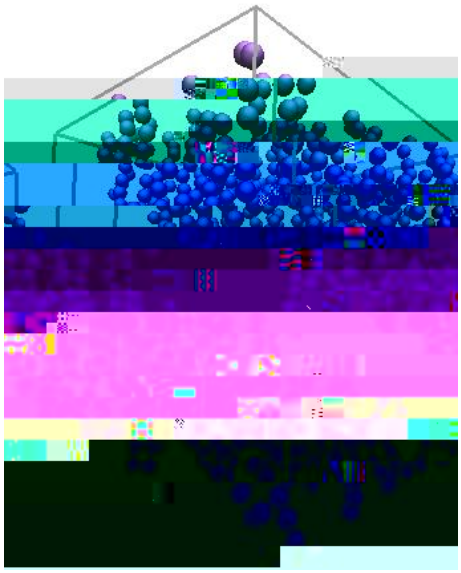

particles remain suspended in Brownian motion under normal conditions whereas those in MR uids settle over time as they are denser than their surrounding uid. As a result the two types of magnetic uid have very di erent applications.

The colloidal properties of ferro uids (the possession of properties of both the liquid and solid states of matter) allow them to be used as seals and lubricants. In particular, they form liquid seals around the spinning drive shafts in hard disks. They also have numerous medical applications including cancer detection and treatment, hypothermia treatment, targeted drug delivery and retina repairs[10,22,24]. Rich et al.[31] recently expressed hope that ferro uids may continue to be exploited in the creation of materials with unique electrical or optical properties (for example, optical tweezers). MR uids, on the other hand, are used in the automotive and aerospace industries in devices such as dampers, shock absorbers, clutches and brakes[16]. They also have military applications in the development of enhanced body armour.

2 Molecular Dynamics

Molecular dynamics is a method for solving Newton's laws of motion that is used in computer simulations of molecular behaviours where intermolecular potentials are involved[1,17]. It can be used to compute the properties of a classical [1] many-body system,[12] such as temperature, energy and shear viscosity[28]

neighbours. Hence for a system of N particles there are $\frac{N(N-1)}{2}$ pairs to be evaluated and so the computation time is $O(N^2)$, although there are techniques that can reduce this time to $O(N)$ (when there are no long range interactions), $O(N^{\frac{3}{2}})$ or at best $O(N \log N)$[12,28,33].
.

$$u_t{}_j^n = \frac{u_j^{n+1} \quad u_j^{n\ 1}}{2 \quad t}; \qquad u_x{}_j^n = \frac{u_{j+1}^n \quad u_j^{n\ 1}}{2 \quad x}:$$

This gives the leapfrog scheme[27,29]

$$\begin{aligned} u_j^{n+1} &= u_j^{n\ 1} \quad a\frac{t}{x} \ u_{j+1}^n \quad u_j^{n\ 1} \\ &= u_j^{n\ 1} \quad u_{j+1}^n \quad u_j^{n\ 1} \end{aligned}$$

where $= a\frac{t}{x}$ is standard notation. This can easily be transformed into the staggered leapfrog method by using information at half steps in space and time instead. The inter-

ment to di erence two large numbers to generate a small number, which would result in loss of precision.

In mathematics predictor-corrector methods tend to be favoured due to the accuracy gained. Such methods operate by using one scheme to perform a calculation and obtain a predicted value. This predicted value is then put into a second, more accurate, scheme to give a corrected value. However, in molecular dynamics simulations such a method is not computationally e cient as it increases the number of calculations that are required.

2.2 Long Range Interactions

Allen and Tildesley[1] de ne long range forces to be those in which the spatial interaction decays at a rate no faster than r^{-d}, where r is the particular separation and d is the dimensionality of the system. Since dipole-dipole interactions in three dimensional space are approximated by r^{-3} they fall into this category. In x3.1 charge-charge interactions are discussed as an introduction to the Ewald method, which are approximated by r^{-1} and hence are long range too.

Such systems can be di cult to represent computationally since for a typical simulation the interaction range of the molecules is much larger than half of the simulation box length. The solution is not as simple as increasing the box size as this would make the cost and computing time required to run a simulation far too great. There are 2 key problems, as described by Hinchli e[17]; the molecules at the edge of the box will be under the in uence of di erent forces to those in a more central position and also, over time, molecules may leave the simulation box and thus reduce the density within.

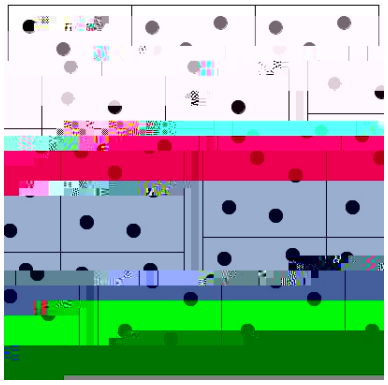

Figure 3: Simpli ed representation of two-dimensional slice of periodic boxes.

These issues can be tackled by creating a system of adjoining simulation boxes that are identical on an atomic level, as demonstrated in Figure 3. Mathematically, this involves simulating the behaviour in one cell and applying periodic boundary conditions (PBCs)

and in the surrounding cells. This resolves the problem of varying influences due to the position of walls as we assume the system is infinite[1,17]. Computing ability is enhanced since we are able to study a microscopic portion of the system and use the PBCs to extrapolate the results throughout the macroscopic system.

The interactions of a molecule with all of its periodic images can be modelled efficiently using Ewald summations[1], which are described in detail in *x*3.

3 Ewald Summations

ticles in the manner discussed in the previous paragraph and includes a proportionality constant of $(4 \quad _0)^{-1}$, where $_0$ is the permittivity (a measure of resistance) of free space[17].Throughout this report all factors of $4 \quad _0$ have been omitted to make the notation compact, as is the convention. This equates to using Gaussian rather than SI units of charge; in this case charge will have units of $mN^{\frac{1}{2}}$ [1].

It is worth noting that the derivation of the Ewald summation takes the periodicity

The relative permittivity of the medium surrounding the sphere containing our summed boxes can di er vastly. For example, a system surrounded by a metal that conducts well has relative permittivity $_s = 1$

where $erfc(x) = \frac{2}{\sqrt{\pi}} \int_x^{\infty} e^{-t^2} dt$ is the complementary error function[1,23], which tends to zero as x increases. Equation (9) gives the amended real space contribution to our potential.

We now have a system of screened charges, as illustrated in Figure 5, consisting of the point charges and the neutralising distribution. So, a second charge distribution needs to be introduced in order to counteract the Gaussian distribution added previously, as depicted in Figure 6 (i.e. Figures 5 and 6 combined leaves just the point charges we require)[1,12,23,28].

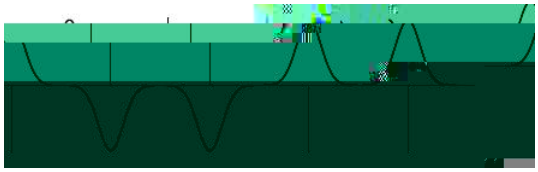

Figure 5: Screened charges.[28]

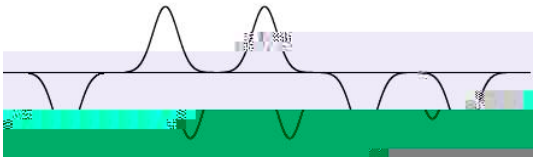

Figure 6: Cancelling distribution.[28]

It may seem easier to simply ignore the contribution of the screening distribution. However, its inclusion means that the summation in (9) converges rapidly and so can be truncated with less loss of accuracy. The speed of convergence is dependent on the width of the Gaussian distribution in (8) as wider distributions will converge more quickly[23]. This can be controlled by selecting an optimal value of the parameter . A further important development is that we can now subtract a cancelling function which can be expressed as a rapidly converging Fourier series. [3]

In order to calculate the contribution from the cancelling charge distribution we start with the periodic sum of Gaussians in (10) at the position of $\mathbf{r}_i$[12].

$$\overset{charge}{G2}(r) = \sum_{j=1}^{N} \sum_{\mathbf{n}} \frac{q_j \, 3e^{-2j\mathbf{r}_{ij}+\mathbf{n}j^2}}{\frac{3}{2}} \qquad (10)$$

We then take the Fourier transform of (10) where $\mathbf{k} = \frac{2\,\mathbf{n}}{L^2} = \frac{2}{L^2}(k_x; k_y; k_z)$ for $k_x; k_y; k_x$ integers is the corresponding vector in reciprocal space[1,12,14,23].

[3] There is a slight abuse of notation in this derivation since i is taken to represent $\sqrt{-1}$ but subscript i still relates to the summation index, as in previous appearances.

$$\hat{G2}^{charge}(k) =$$

rewrite it as

$$U_c^k = \frac{2}{L^3} \sum_{\mathbf{k}\neq\mathbf{0}} \sum_{i=1}^{N} \sum_{j=1}^{N} \frac{q_i q_j}{k^2} e^{-\frac{k^2}{4\alpha^2}} \cos(\mathbf{k} \cdot \mathbf{r}_{ij}) \tag{15}$$

where we have ignored the imaginary sin term since we need to be able to perform computations in real space[23]. Since the number of terms required in (15) increases as the Gaussian distribution gets wider it is important to balance the real space and reciprocal space sums to achieve optimal accuracy. Generally, α is set to be $\frac{5}{L}$ and 100-200 vectors $\mathbf{k}$ are used[1,23].

When introducing the cancelling distribution cloud described in (10) we included self-interaction terms, which we excluded from the real space sum using the $\sum'$ notation. So, a further correction term is required to counteract this. The charge distribution that we have over counted by is

$$\rho_{G3}^{charge}(r) = \frac{q_i \alpha^3 e^{-\alpha^2 r^2}}{\pi^{\frac{3}{2}}}.$$

Using Poisson's equation as we did in the derivation of U_c^k we can work out the contribution of this to the overall potential. Using the spherical geometry of the cancelling charge cloud we can use Poisson's equation in the following form[12]: $\nabla^2 r^2$

this end we have

$$\rho_2^{charge}(r = 0) = \frac{2q_i}{p=}:$$

Hence the self contribution to the potential is given by[12,23]

$$U_c^{self} = \quad p= \sum_{i=1}^{N} q_i^2: \tag{17}$$

The same result can be obtained by using the Fourier space term given in (15) and setting $i = j$.

Combining the four terms; (6), (9), (15) and (17); discussed in this section gives the nal expression

$$U_c(\ _s = 1) = U_c^r + U_c^k + U_c^{self} + U_c^{surf}$$
$$= \sum_{i=1}^{N}\sum_{j=1}^{N} q_i q_j \quad \frac{1}{2} \quad \sum_{\mathbf{n}2\mathbb{Z}^3} {}^{0}\frac{erfc(\ j\mathbf{r}_{ij} + \mathbf{n}j)}{j\mathbf{r}_{ij} + \mathbf{n}j} \quad + \frac{2}{L^3} \sum_{\mathbf{k}\in\mathbf{0}} \frac{1}{k^2} e^{\ \frac{k^2}{4\ ^2}} \cos(\mathbf{k} \quad \mathbf{r}_{ij}) \quad \Bigg]$$

2q031

$$\sum_{i=1}^{N} q_i^2$$

a system surrounded by a vacuum is[1,33]

$$U_d^{surf} = \frac{2}{3L^3} \sum_{i=1}^{N} \sum_{j=1}^{N} \quad _i \quad _j : \tag{20}$$

Combining the slow converging summation in (19) with a suitable neutralising Gaussian distribution we get the following real space contribution to our potential[1,33]:

$$U_d^r = \frac{1}{2} \sum_{\mathbf{n} 2 \mathbb{Z}^3}{}' \sum_{i=1}^{N} \sum_{j=1}^{N} (\quad _i \quad _j) B(j r_{ij} +$$

$$U_d(\ _s = 1) = U_d^r + U_{d_{\blacksquare}}^k + U_d^{self} + U_d^{surf}$$

$$= \sum_{i=1}^{N} \sum_{j=1}^{N} \frac{1}{2} \sum_{\mathbf{n} 2 \mathbb{Z}^3} 0 (\ _i \quad _j) B(j\mathrm{r}_{ij} + \mathrm{n}j) \quad (\ _i \quad (\mathrm{r}_{ij} + \mathrm{n}))(\ _j \quad (\mathrm{r}_{ij} + \mathrm{n})) C(j\mathrm{r}_{ij} + \mathrm{n}j)$$

$$+ \frac{2}{L^3} \sum_{\mathbf{k} 2 \mathbb{Z}^3; \mathbf{k} \neq \mathbf{0}}$$

Taking the Fourier transform of (25) and integrating gives

$$\mathcal{F}f(\ ) = \sum_{n=\ 1}^{\infty} f(n\ \ r)e^{\ 2i\ \ n\ \ r} \tag{26}$$

for some $\ 2\ \mathbb{R}$. We can truncate the sum in (26) by assuming that $f(r) = 0$ unless $0\ \ n < M$ for a su ciently large M so that

$$\mathcal{F}f(\ ) = \sum_{n=0}^{M-1} f(n\ \ r)e^{\ 2i\ \ n\ \ r}:$$

This equation now contains M pieces of information that need to be evaluated at points $= \frac{k}{M\ \ r}$ for $k = 0;\ \ ;M$ [14]. So, the discrete Fourier transform (DFT) is taken to be

$$F(k) = \mathcal{F}f\left(\frac{k}{M\ \ r}\right) = \sum_{n=0}^{M-1} f(n\ \ r)e^{\ \frac{2i\ \ nk}{M}}: \tag{27}$$

However, in (27) many values are calculated twice and it is by preventing this that the FFT makes computation quicker. If we take M to be even we can split the sum in (27) into its even and odd components as shown below.

$$\begin{aligned} F(k) &= F_{even}(k) + F_{odd}(k) \\ &= \sum_{n=0}^{\frac{M}{2}-1} f((2n)\ \ r)e^{\ \frac{2i\ \ (2n)k}{M}} + \sum_{n=0}^{\frac{M}{2}-1} f((2n+1) \end{aligned}$$

and

$$e^{\ i\ (2n+1)} = \cos(\quad (2n+1)) + i\sin(\quad (2n+1))$$
$$= \quad 1 + 0 = \quad 1:$$

So, (29) becomes

$$F\quad k + \frac{M}{2}\quad = \sum_{n=0}^{\frac{M}{2}X\ 1} f((2n)\quad r)e^{\ \frac{2i\ \ (2n)k}{M}} \quad \sum_{n=0}^{\frac{M}{2}X\ 1} f((2n+1)\quad r)e^{\ \frac{2i\ \ (2n+1)k}{M}}$$
$$= F_{even}(k)\quad F_{odd}(k): \qquad (30)$$

It is the relationship between $F(k)$ and $F\quad k + \frac{M}{2}$

Hence, in order to find the force, $\mathbf{F}_i$, acting on a particular particle, i, we need to take U for that particle and differentiate with respect to $\mathbf{r}_i$.

Due to the complexity of the equation it is easier to tackle this task component by component; i.e. $\mathbf{F}_i = \frac{@(U_i)}{}$

follows:

$$
\begin{aligned}
F_i^r = & \sum_{j=1}^{N} \sum_{\mathbf{n} \in \mathbb{Z}^3}{}' (q_i q_j)\left[(\mathbf{r}_{ij} + \mathbf{n})C(j\mathbf{r}_{ij} + \mathbf{n}j) - B\right] \\
& + C(j\mathbf{r}_{ij} + \mathbf{n}j)(q_j[\mu_i \cdot (\mathbf{r}_{ij} + \mathbf{n})] + q_i[\mu_j \cdot (\mathbf{r}_{ij} + \mathbf{n})]) \\
& + [\mu_i \cdot (\mathbf{r}_{ij} + \mathbf{n})][\mu_j \cdot (\mathbf{r}_{ij} + \mathbf{n})][C - (\mathbf{r}_{ij} + \mathbf{n})D(j\mathbf{r}_{ij} + \mathbf{n}j)] \\
= & \sum_{j=1}^{N} \sum_{\mathbf{n} \in \mathbb{Z}^3}{}' f(q_i q_j)(\mathbf{r}_{ij} + \mathbf{n}) + q_j[\mu_i \cdot (\mathbf{r}_{ij} + \mathbf{n})] + q_i[\mu_j \cdot (\mathbf{r}_{ij} + \mathbf{n})]gC(j\mathbf{r}_{ij} + \mathbf{n}j) \\
& - [\mu_i \cdot (\mathbf{r}_{ij} + \mathbf{n})][\mu_j \cdot (\mathbf{r}_{ij} + \mathbf{n})](\mathbf{r}_{ij} + \mathbf{n})D(j\mathbf{r}_{ij} + \mathbf{n}j) \qquad (33)
\end{aligned}
$$

since we can eliminate the scalar terms. Notice that we were able to ignore the modulus(r)]TJ/F3]331

position of i using the following relationship

$$_i = \quad _i \quad E_i$$

where $E_i = \frac{@(U_i)}{@ \ _i}$. As with force we will calculate the torque one component at a time. Clearly there is again no contribution from the self term. So, calculating the torque contribution in real space for a particular i yields

$$E_i^r = \frac{@(U_i^r)}{@ \ _i}$$

$$= \sum_{\mathbf{n}2\mathbb{Z}^3} \sum_{j=1}^{N} \frac{@}{@ \ _i} (\ _i \quad _j)B(jr_{ij} + nj) \quad (\ _i \ (r_{ij} + n))(\ _j \ (r_{ij} + n))C(jr_{ij} + nj)$$

$$= \sum_{\mathbf{n}2\mathbb{Z}^3} \sum_{j=1}^{N} \quad _jB(jr_{ij} + nj) \quad (r_{ij} + n)(\ _j \ (r_{ij} + n))C(jr_{ij} + nj)$$

$$) \quad _i^r = \sum_{\mathbf{n}+_j} (0$$

Finally the surface term contribution is

$$\begin{aligned}
\mathbf{E}_i^{surf} &= \frac{\partial(U_i^{surf})}{\partial \quad _i} \\
&= \frac{4}{3L^3} \sum_{j=1}^{N} \frac{\partial}{\partial \quad _i} \quad _i \quad _j \\
&= \frac{4}{3L^3} \sum_{j=1}^{N} \quad _j \\
{}_i^{surf} &= \frac{4}{3L^3} \sum_{j=1}^{N} \quad _i \quad _j : \qquad (37)
\end{aligned}$$

Combining the three terms; (35), (36) and (37); to obtain the overall torque we get

$$\begin{aligned}
{}_i &= {}_i^{r} + {}_i^{k} + {}_i^{surf} \\
&= \sum_{j=1}^{N} \sum_{\mathbf{n} \in \mathbb{Z}^3}{}' \quad (\quad _i \quad \quad _j) B(jr_{ij} + \mathbf{n}j) \quad \quad _i \quad (r_{ij} + \mathbf{n})(\quad _j \quad (r_{ij} + \mathbf{n})) C(jr_{ij} + \mathbf{n}j) \\
&\quad + \frac{4}{L^3} \sum_{\substack{\mathbf{k} \in \mathbb{Z}^3 \\ \mathbf{k} \neq \mathbf{0}}} \frac{1}{k^2} (\quad _i \quad \mathbf{k})(\quad _j \quad \mathbf{k}) e^{\left(-\frac{k}{L}\right)^2} \cos(\mathbf{k} \quad r_{ij}) + \frac{1}{3} \sum_{j=1}^{N} \quad _i \quad \quad _j \quad :
\end{aligned}$$

3.3 Errors in Ewald Summations

As with the previous section we are only concerned with dipolar interactions, since these are the ones present in magnetic fluids. As such we will again omit the subscript *d* when discussing various elements in order to keep notation simple.

Wang and Holm[33] derived and successfully tested estimates for the errors in the Ewald summation derived for dipoles in *x*3.1.2 and also the forces and torques given in *x*3.2. All of the equations and results discussed in this section are taken from their work.

As described in *x*3.2 there are two cut-offs; one in real space, r_c, and one in reciprocal space, k_c. So, there are errors in real space and reciprocal space, which we assume to be independent of each other. There are no errors in the surface or self terms since there are no truncations in these. Due to the assumption of independence of errors we can write the total cut-off error for the Ewald summation as

$$= \sqrt{(\quad ^{r})^2 + (\quad ^{k})^2}$$

where represents U, F and .

In molecular dynamics accuracy is generally tested using the root mean square (rms)

error in the forces:

$$F = \sqrt{\frac{1}{N}\sum_{i=1}^{N}(\quad F_i)^2} = \sqrt{\frac{1}{N}\sum_{i=1}^{N}(F_i \quad F_i^{exact})^2} \tag{38}$$

where F_i is the force on particle i calculated by the Ewald summation and F_i^{exact} is the exact force on that particle. This method will be employed throughout this section,

where $_{jm}$ is the Kronecker delta function, which equals one if $j = m$ and zero otherwise. The change of notation in (41) comes about because the mean square force error for two dipoles, $h(\ ^{r}_{ij})^2 i$, is no longer dependent on i and j.

Combining the results in (39) and (41) we look at the average over all particle con gurations of the squared real space error:

$$h(\ \mathrm{F}^{r}_{i})^2 i = \ ^{2}_{i} \sum_{j \in i} \sum_{m \in i} j\ _{j} j j\ _{m} j h\ ^{r}_{ij}\ \ ^{r}_{im} i$$

$$= \ ^{2}_{i} \sum_{j=1}^{N} \ ^{2}_{j} (\ ^{r})^2 \qquad (42)$$

Substituting the approximation

$$* \sqrt{\frac{1}{N} \sum_{i=1}^{N} (\ \mathrm{F}_i)^2} + \sqrt{\frac{1}{N} \sum_{i=1}^{N} h(\ \mathrm{F}_i)^2 i}$$

into (38) and using the term derived in (42) we can get an expression for the con gurational average value $h\ \ F i$.

$$h\ \ F i \quad \sqrt{\frac{1}{N} \sum_{i=1}^{N} \ ^{2}_{i} \sum_{j=1}^{N} \ ^{2}_{j} (\ ^{r})^2}$$

$$) \quad F \quad p\overline{\frac{1}{N}} \sum_{j=1}^{N} \ ^{2}_{j}\ ^{r} \qquad (43)$$

From the de nition of $\ ^{r}_{ij}$ we can approximate $(\ ^{r})^2$. Let $\hat{}$ and $\hat{}^{0}$ be two unit orientation vectors of arbitrary dipoles. Then choosing the z axis of the spherical coordinate system $(r; \ ; \ )$ to be along $\hat{}$ means that $! (\hat{}; \hat{}) = \ $. Furthermore,

$$\cos ! (\hat{}^{0}; \hat{}) = \cos \ \cos ! (\hat{}; \hat{}^{0}) + \sin \ \sin ! (\hat{}; \hat{}^{0}) \cos \ :$$

Using all of this information in conjunction with (40) gives

$$(\ ^{r})^2 \quad \frac{1}{L^3} \int_{r_c}^{1} r^2 \mathrm{d}r \int_{0} \sin \ \mathrm{d} \int_{0}^{2} \mathrm{d} \ [\hat{} \cos ! (\hat{}; \hat{}^{0}) + \hat{}(\cos \ \cos ! (\hat{}; \hat{}^{0})$$

$$+ \sin \ \sin ! (\hat{}; \hat{}^{0}) \cos \ ) + \hat{}^{0} \cos \ ] r C(r) \quad \hat{}$$

$$\langle \sin^2 i \rangle = \langle \cos^2 i \rangle = \frac{1}{2}; \qquad \langle \sin i \cos i \rangle = 0: \tag{44}$$

These results can be substituted into our expression for $(\Delta_r)^2$ reducing the equation to a more manageable format. Wang and Holm[33] then make further simplifications by applying the asymptotic expansion formula. This leads to the following approximation to $(\Delta_r)^2$:

$$(\Delta_r)^2 \approx \frac{\frac{13}{6}C_c^2 + \frac{2}{15}D_c^2 \quad \frac{13}{15}C_c D_c}{L^3 r_c^9 \quad ^4} e^{-\quad ^2 r_c^2} \tag{45}$$

where

$$C_c = 4 \quad ^4 r_c^4 + 6 \quad ^2 r_c^2 + 3;$$
$$D_c = 8 \quad ^6 r_c^6 + 20 \quad ^4 r_c^4 + 30 \quad ^2 r_c^2 + 15:$$

Taking the square root of (45) and substituting the result into (43) gives

$$\Delta F_r \approx \sum_{j=1}^{N} q_j^2 e^{-\quad ^2 r_c^2} \sqrt{\frac{\frac{13}{6}C_c^2 + \frac{2}{15}D_c^2 \quad \frac{13}{15}C_c D_c}{L^3 r_c^9 \quad ^4 N}} \tag{46}$$

The real space cut-off error in the torque is derived by following the same method used for the force cut-off error, which results in (47).

$$\Delta_r \approx \sum_{j=1}^{N} q_j^2 e^{-\quad ^2 r_c^2} \sqrt{\frac{\frac{1}{2}B_c^2 + \frac{1}{5}C_c^2}{L^3 r_c^7 \quad ^4 N}} \tag{47}$$

with

$$B_c = 2 \quad ^2 r_c^2 + 1$$

and C_c as stated before.

Whilst the derivation for the real space cut-off error for the total potential energy is also calculated in the same way as the force there is a small difference. Since the interaction energy between two dipoles is split equally between them the sum of the mean square contains each pair's contribution twice in this case. Thus, the error is taken to be half of this sum.

$$\Delta U_r \approx \sum_{j=1}^{N} q_j^2 e^{-\quad ^2 r_c^2} \sqrt{\frac{\frac{1}{4}B_c^2 + \frac{1}{15}C_c^2 \quad \frac{1}{6}B_c C_c}{L^3 r_c^7 \quad ^4 N}} \tag{48}$$

The cut-off errors given in (46), (47) and (48) all contain the exponential

$e^{-2} = 5 \times 10^{-5}$ to get the following simplified versions:

$$F^r = 8\left(\frac{4}{}\right)^{2} \sum_{j=1}^{N} q_j^2 e^{-\alpha^2 r_c^2} \sqrt{\frac{2r_c^3}{15NL^3}},$$

$$^r = 4\left(\frac{2}{}\right)^{2} \sum_{j=1}^{N} q_j^2 e^{-\alpha^2 r_c^2} \sqrt{\frac{r_c}{5NL^3}},$$

$$U^r = 4\left(\frac{2}{}\right)^{2} \sum_{j=1}^{N} q_j^2 e^{-\alpha^2 r_c^2} \sqrt{\frac{r_c}{15NL^3}}.$$

An advantage of this format is that it makes it easier to determine how the error depends on the parameters r_c and , which is useful when deciding how to optimise them as discussed in *x*3.3.3.

3.3.2 Errors in Reciprocal Space

Further to the assumptions made in *x*3.3.1 we now assume that the radial distribution function of the particles, which represents the variation in density as a function of the distance from a certain particle, approximates to unity at all distances.

From the reciprocal space force term (34) we can see that the reciprocal space cut-o in the error of the force acting on particle i is given by

$$F_i^k = \sum_{j=1}^{N} \sum_{\mathbf{k}\,k>k_c} \frac{4\,\mathbf{k}}{L^3k^2}(\quad_i\quad \mathbf{k})(\quad_j\quad \mathbf{k})e^{-(\frac{k}{L})^2} \sin(\mathbf{k}\quad \mathbf{r}_{ij}). \tag{49}$$

In (49) t iagonal term (when $j = i$) in the sum is not reliant on the positioning of the particles so provides a systematic contribution to the reciprocal cut-o error. In the force and que cut-o errs error. I0 1 344.925 i22 .[()()]TJ/F53(I0 1 344.925 i22 .[()TJ/-407atic)-316

jer81 9.425 ;2 Tf 5.977 0 Td [(k)]T86itN

where $\hat{\mathbf{k}}$ is a unit vector along $\mathbf{k}$ and the sin term has been rewritten using the identity given in (4) and the symmetrical nature of the summation over $\mathbf{k}$. Once more assuming that the positions and orientations are random gives us the following result

$$\langle (F_i^k)^2 \rangle = \sum_{j \neq i} \sum_{m \neq i} q_j q_m \langle T_{ij}^k T_{im}^k \rangle$$
$$= q_i^2 \sum_{j=1}^{N} q_j^2 (\xi^k)^2$$

where again ξ^k does not depend on i or j and δ_{jm} is the Kronecker delta function.

As before we use the de nition of T_{ij}^k to write

$$(\xi^k)^2 \quad \frac{4}{L^3} \int_{k_c/2}^{\infty} e^{-2(\frac{k}{L})^2} k^4 dk \int_0^{\pi} \sin \theta \, d\theta$$
$$\int_0^{2\pi} \cos^2 \phi \, [\cos \phi \cos \theta \, I(\hat{\mathbf{k}}; \hat{\mathbf{k}}^0) + \sin \phi \sin I(\hat{\mathbf{k}}; \hat{\mathbf{k}}^0) \cos \phi]^2 d\phi \; . \qquad (51)$$

Applying the same process as in the derivation of the real space cut-o error Wang and Holm[33] simplify (51) to give

$$(\xi^k)^2 \quad \frac{128 \pi^2 \alpha^2 k_c^3}{15 L^5} e^{-2(\frac{k_c}{L})^2}.$$

Hence, the reciprocal space cut-o error in the forces is

$$F^k \quad \frac{4}{L^2} \sum_{j=1}^{N} q_j^2 e^{-(\frac{k_c}{L})^2} \sqrt{\frac{2 k_c^3}{15N}}. \qquad (52)$$

where we have not distinguished between diagonal and o diagonal contributions since the diagonal contribution is zero in this case.

Calculating the reciprocal space cut-o error for torque in the same way as for force and ignoring the zero diagonal contribution gives

$$\tau^k \quad \frac{4}{L^2} \sum_{j=1}^{N} q_j^2 e^{-(\frac{k_c}{L})^2} \sqrt{\frac{k_c}{5N}}.$$

Following this method again the reciprocal space error in the total interaction potential is calculated, taking into account the systematic contribution from the diagonal term. As was the situation in the real space case the sum of the mean square of the total interaction energy double counts each pair of interactions and this has been taken into account to get the following results:

where

$$U^k_{off} \quad \frac{4}{L^2} \sum_{j=1}^{N} {}^2_j e^{-(\frac{k_c}{L})^2} \sqrt{\frac{k_c}{15N}}$$

$$U^k_{diag} = \frac{1}{2\pi\sqrt{N}} \sum_{i=1}^{N} \sum_{\mathbf{k}, k>k_c} \frac{4}{L^3} {}^2_i e^{-(\frac{k_c}{L})^2} \cos^2 !(\hat{}_i; \hat{k})$$

$$\frac{2}{L^3\pi\sqrt{N}} \sum_{j=1}^{N} {}^2_j \int_{k_c}^{1} e^{-(\frac{k_c}{L})^2 k^2} dk \int_0^{} \sin \, d \int_0^{2} \cos^2 \, d$$

$$\frac{4}{3L} \frac{{}^2 k_c}{\pi\sqrt{N}} \sum_{j=1}^{N} {}^2_j e^{-(\frac{k_c}{L})^2}:$$

Comparing the diagonal and o diagonal terms we can see that the systematic contribution to the reciprocal space error is a factor of $L\sqrt{k_c}$ larger than the o -diagonal term. Since this is much greater than one this term dominates the reciprocal space error in the total interaction energy.

3.3.3 Optimising the Parameters

Wang and Holm[33] give the overall computing time required for using the Ewald summation to calculate the forces as

$$T = a_r N^2 \left(\frac{r_c}{L}\right)^3 + a_k N k_c^3$$

where a_r and a_k can only be determined through numerical work and depend on how the code is implemented. The numerical work carried out by Wang and Holm[33] (in which they used standard Fourier transforms rather than FFTs) found them to be $a_r = 2{:}5$ s and $a_k = 0{:}7$ s for their implementation and so we shall proceed using these values. Using

Substituting these into the equation for overall computation time alongside the values for a_r and a_k and di erentiating with respect to gives:

$$T \quad 2{:}5N^2 \quad \frac{p\overline{\ln}}{L}^{!3} \quad 0{:}7N(B \quad p\overline{\ln})^3$$

$$) \quad \frac{T}{} \quad 7{:}5N^2 \quad \frac{(p\overline{\ln})^3}{L^3 \ 4}^{!} \quad 2{:}1N(B \ p\overline{\ln})^3 \ ^2{:}$$

Setting this equal to zero in order to nd the minimum value of we see that $/ N^{\frac{1}{6}}$, which means that $k_c / N^{\frac{1}{6}}$ as well and $r_c / N^{\frac{1}{6}}$. If the parameters are chosen in this way the overall computation time becomes proportional to $N^{\frac{3}{2}}$ where the required accuracy decides the proportionality constant[33].

4 Simulation

The code controlling the simulation run in this section is all written in the C programming language and was provided by Dr. Zuowei Wang of the University of Reading (supervisor for this project). As a result its implementation is not discussed here.

The details of nely controlled simulations run from this code have been published previously[19,33]. However, for this project further simulations were run to provide a cursory visualisation of the behaviours of ferro uids discussed in *x*1 and demonstrate some of the ideas discussed in this report. This required a basic knowledge of the code involved, particularly how to adjust the various parameters in the program to achieve the desired result. Visual Molecular Dynamics (VMD) software was also utilised to produce the diagrams that are included in this section[18]. Finally, since the output from the original code was not in the required format two trivial programs in C^{++} were created to convert output from the simulation into one format that could be graphed and one that was compatible with the VMD software. The diagrams in this section only show one simulation box; remember that we are dealing with a system of adjoining boxes displaying identical behaviour.

to consider dipoles as part of the same cluster when the dipolar interaction energy is less than a value predetermined by

$$U_{bond} = \quad 1{:}4 \;\; k_B T$$

where is the dipolar coupling constant (= 4 in this case) and $k_B T$ is the temperature measured in Kelvin (= 1 in this case)[19,35]. This is equivalent to 70% of the dipolar interaction energy between two touching particles with their dipole moments perfectly aligned. The average cluster size is then taken to be

$$\langle S \rangle = \frac{\sum_s s n_s}{\sum_s n_s}$$

where n_s is the number of clusters that have size s[19,35].

Cluster size is something that cannot be measured in experimental work and so this highlights the importance of simulations in enabling scientists to see more than they can in a lab. Kantorovich et al.[21] go into detail about the struggle of experimental work to even obtain proof of the chain formations recognised so easily in simulative works. Many other researchers have published articles in recent years regarding the aggregation (formation of clusters) of magnetic uids, so data such as that taken from this simulation are an invaluable contribution to the eld[8,9,30].

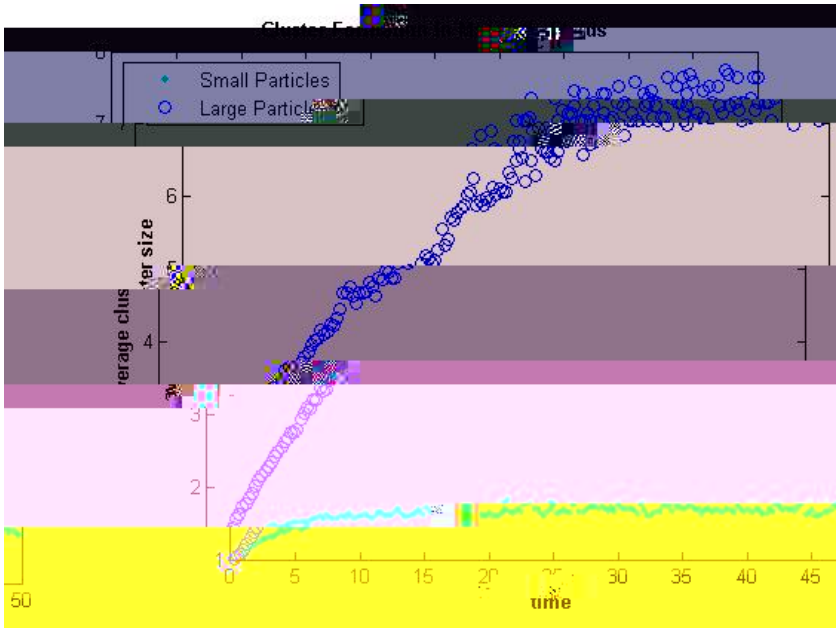

Figure 7: Comparison of average cluster size over time for large and small particles after the application of external magnetic eld.

Since we are starting from a random con guration of the particles we would expect the average cluster size to take value 1 at time $t = 0$. This is clearly evident in Figure

particles respectively, and we can see that the set-up indeed appears to be random. In Figures 9 and 11 we can see the position of the particles at the end of the simulation. Although the chain formation is evident in both sets of particles there is clearly more structure in the system of larger particles. The graph veri es this as we can see that the large particles form clusters four times the size of the small particles in the equivalent time frame. This demonstrates how essential the de nition of touching stated earlier is since in Figure 9 the clusters appear to be much larger for small particles than the data indicates. Also, from Figure 7 we can see how soon after the external eld is applied aggregation begins.

It may appear in Figure 7 that there are several measurements taken at some time steps. This is not the case; it is simply a result of the scale of the graph in comparison to the size of the time step.

5 Dealing with a Confined Geometry

The Ewald method discussed in *x*3 is designed for application to a standard three dimensional geometry. In this section the method is adapted to enable its use in a geometry that is confined in one direction (called a slab geometry). The method used previously is no longer valid in this situation since periodicity in the confined direction is lost and the formulae were derived assuming periodicity in all three directions.

Slab geometries are found in many scenarios of interest to physicists and chemists including fluids contained between two walls, electrolyte solutions between charged surfaces and transport through membranes[2,6]. More interestingly in relation to this project, slab geometries are also characteristic of thin films of ferrofluids, such as those simulated in *x*4.

5.1 What is a Confined Geometry?

In order to create a confined, or slab, geometry we start with the standard three dimensional periodic system discussed in *x*2.2 and insert two planes parallel to the top and bottom of the simulation cube. The substance being modelled (magnetic fluids in our case) is then contained between these walls, as demonstrated very crudely in Figure 12. So, when we model our system the strips containing the fluid are now infinitely periodic in only two directions and are finite in the third. This leads to the creation of what is termed a 2D+*H* system; i.e. two dimensions are as before but the third is restricted according to the height, *H*, of the strips containing fluid.

Throughout this section the word `strip' is used to represent the cuboids that the simulation fluid is contained in and `gap' refers to the spaces in between the strips that are empty. The term `standard geometry' refers to the three dimensional periodic system we looked at in *x*3 whilst both `slab geometry' and `confined geometry' describe the new 2D+*H* setup.

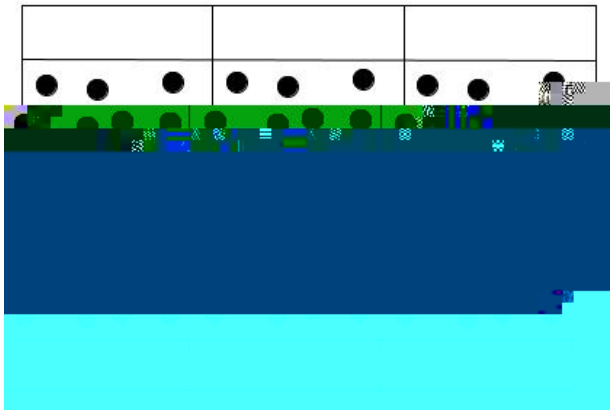

Figure 12: Simplified two-dimensional representation of confined geometry set up.

potential (see also Arnold et al.[2]):

$$U_c^{slabsum} = \frac{2\pi}{V} M_z^2 \tag{55}$$

where $V = L_x L_y L_z$ is the volume of a simulation box and $M = \sum_{k=1}^{N} q_k \mathbf{r}_k$ with M_z being the z component of this. This results in the summation being performed slab-wise rather than the spherical manner considered before, which is far more useful. Slab-wise summation means that we first consider the original strip by adding images of the original simulation box in the x and y axes directions and then add simulation boxes in symmetrical pairs (above and below) in the z axis direction. This new term already takes into account the change of behaviour at the surface of the system and so the surface term used in x3.1 is no longer required. On inspection the similarities between this term and the surface term used previously are obvious.

The real space part of the Ewald summation is almost identical in a slab geometry to the standard three dimensional set-up. It is given by

$$U_c^{slabr} = \frac{1}{2} \sum_{\mathbf{n} \in \mathbb{Z}^2}{}' \sum_{k=1}^{N} \sum_{j=1}^{N} q_k q_j \frac{erfc(\alpha |\rho_{kj} + \mathbf{n}; z_{kj}|)}{|\rho_{kj} + \mathbf{n}; z_{kj}|}$$

where ρ_{kj} describes the projection of $\mathbf{r}_{kj}$ onto the $(x;y)$ plane and $\mathbf{n} = (n_x L_x; n_y L_y)$. In fact by clever choice of

expression in (57) is basically the same as the Fourier term in our previous derivation with k and k replaced by G and G respectively. From the de nition of G we can see that this makes sense.

Now that we have amended our Ewald summation from $x3$ to t our new geometry we need to subtract the inter-strip interactions from our total potential. Brodka[4] takes the di erence between the reciprocal space term for a two dimensional system and the equivalent term derived in three dimensions. Then analysis of the convergence of each term in the resulting expression is discussed in order to simplify it. This yields the following expression for the ELC term[4{6]:

$$U_c^{ELC} = \frac{1}{L_x L_y} \sum_{\mathbf{G} \neq 0} \frac{1}{G\,(e^{G L_z} - 1)} \sum_{k=1}^{N} \sum_{j=1}^{N} S_{c+;k}(\mathbf{G})\, S_{c\ ;j}(\mathbf{G}) + S_{c\ ;k}(\mathbf{G}\,\mathbf{G}$$

term for dipole-dipole interactions[5,7,15].

$$U_d^{slabk} = \frac{2}{V} \sum_{\mathbf{G}\neq 0} \sum_{k=1}^{N} \sum_{j=1}^{N} (\quad_k \quad \mathbf{G})(\quad_j \quad \mathbf{G}) \frac{1}{G^2} e^{\quad \frac{G^2}{4\quad^2}} \cos(\mathbf{G} \quad \mathbf{r}_{kj}) \tag{59}$$

The term correcting for the change in summation technique takes the same form as (55) but the de nition of M has changed. So, we have

$$U_d^{slabsum} = \frac{2\quad M_z^2}{V} \tag{60}$$

where $M^2 = \sum_{k=1}^{N} \sum_{j=1}^{N} \quad_k \quad_j$ and M_z^2 is again the z component of this.

In the new ELC term for dipolar interactions the only change is to the format of the functions $S\quad_{;k}(\mathbf{G}\quad)$ and $S\quad_{;j}(\mathbf{G}\quad)$.

$$U_d^{ELC} = \quad \frac{}{L_x L_y} \sum_{\mathbf{G}\neq 0} \frac{1}{G\ (e^{G\quad L_z} \quad 1)} \sum_{k=1}^{N} \sum_{j=1}^{N} S_{d+;k}(\mathbf{G}\quad) S_{d\quad;j}(\mathbf{G}\quad) + S_{d\quad;k}(\mathbf{G}\quad) S_{d+;j}(\mathbf{G}\quad) \tag{61}$$

where

$$S_{d\quad;k}(\mathbf{G}\quad) = (i\quad_k \quad \mathbf{G} \qquad \quad^z_k \quad G\quad) e^{i\mathbf{G}\quad\quad_k} e^{\quad G\quad z_k};$$

and

$$S_{d\quad;j}(\mathbf{G}\quad) = (\quad i\quad_j \quad \mathbf{G} \qquad \quad^z_j \quad G\quad) e^{\quad i\mathbf{G}\quad\quad_j} e^{\quad G\quad z_j}:$$

In the above result $\quad_k$ and $\quad^z_k$ denote components of the dipole moment $\quad_k$ that are parallel and perpendicular to the $(x;y)$ plane respectively. Combining all the terms discussed in this section ((21), (59), (23), (60) and (61)) gives the overall dipole-dipole potential in a con ned geometry. [7]

$$\begin{aligned} U_d^{slab} &= U_d^r + U_{d\_}^{slabk} + U_d^{self} + U_d^{slabsum} + U_d^{ELC} \\ &= \sum_{k=1}^{N} \sum_{j=1}^{N} \frac{1}{2} \sum_{\mathbf{n}\in\mathbb{Z}^3}{}' (\quad_k \quad_j) B(j\mathbf{r}_{kj} + \mathbf{n}j) \quad (\quad_k \quad (\mathbf{r}_{kj} + \mathbf{n}))(\quad_j \quad n \end{aligned}$$

SX

A direct comparison with the Ewald method derived for dipolar interactions in a three dimensionally periodic system indicates that the main change is the addition of the final term. The only other differences are the change of notation in the reciprocal space term and the requirement to deal with the z component only in the final term. An additional consideration is that must be chosen in such a way as to keep the real space summation within the simulation box to avoid complicating this term.

5.3 Application of Ewald Method for a Confined Geometry

As we did when looking at the standard three dimensional Ewald summation we are only going to look at applications and errors in relation to dipolar interactions, so we will drop the subscript d from our notation. All of the considerations to be made when programming the three dimensional Ewald summation remain the same for a slab geometry. It is simply the terms involved that have changed. As a result the program used in *x*4 could be utilised to simulate the new geometry with only minor changes required. These are, chiefly, the addition of the extra term in the Ewald summation and the introduction of the walls into the program.

Clearly since we are using the same real space term as in the standard geometry the force and torque for this term will be the same as those given in *x*3.2. The self term is also the same as was used in the standard three dimensional geometry and hence it once again does not contribute to either the force or the torque.

The discussions in this section relating to the contribution of the new ELC and summation terms to the force and torque are only preliminary. I was unable to find any publications that have calculated them previously and due to time constraints have been unable to carry out any numerical work to examine their accuracy.

5.3.1 Force

As discussed in *x*3.2.1 the force, $\mathbf{F}_k$, acting on a particular particle, k is found by differentiating U^{slab} with respect to $\mathbf{r}_k$ and negating the answer. We can state the force contribution in reciprocal space directly as a result of the similarities between (59) and (22):

$$\mathbf{F}_k^{slabk} = \frac{4}{V} \sum_{j=1}^{N} \sum_{\substack{\mathbf{G} \in \mathbb{Z}^3 \\ \mathbf{G} \neq \mathbf{0}}} \frac{\mathbf{G}}{G^2} e^{-(\frac{G}{L})^2} (q_k \mathbf{G})(q_j \mathbf{G}) \sin(\mathbf{G} \cdot \mathbf{r}_{kj}).$$

There is no contribution to the force from the summation method term, since it is not dependent on the position of individual particles. Hence, it only remains to calculate the ELC term's contribution to the overall force. Although $\mathbf{r}_k$ is not explicitly present in this

term it is contained within $_k$, its representation in the $(x;y)$ plane. So we have

$$
\begin{aligned}
\mathbf{F}_k^{ELC} &= \frac{@(U_k^{ELC})}{@\mathbf{r}_k} \\
&= \frac{@(U_k^{ELC})}{@\ _k}\hat{\ }_k \quad \frac{@(U_k^{ELC})}{@z_k}\hat{z}_k \\
&= \frac{2}{L_x L_y} \sum_{\mathbf{G}\neq 0} \frac{1}{G\ (e^{G\ L_z} \quad 1)} \sum_{j=1}^{N} \frac{@}{@\ _k}\ S_{+;k}(\mathbf{G}\ )S_{\ ;j}
\end{aligned}
$$

Finally, we look at the torque contribution from the ELC term added to allow us to work in this geometry:

$$
\begin{aligned}
\mathbf{E}_k^{ELC} &= \frac{\partial(U_k^{ELC})}{\partial \quad_k} \\
&= \frac{\partial(U_k^{ELC})}{\partial \quad_k}\,\mathbf{c}_k \quad \frac{\partial(U_k^{ELC})}{\partial \quad_k^z}\,\mathbf{c}_k^z \\
&= \frac{2}{L_x L_y} \sum_{\mathbf{G}\neq 0} \frac{1}{G\,(e^{G\ L_z} \quad 1)} \sum_{j=1}^{N} \frac{\partial}{\partial \quad_k} \left[S_{+;k}(\mathbf{G})S_{\ ;j}(\mathbf{G}) + S_{\ ;k}(\mathbf{G})S_{+;j}(\mathbf{G}) \right] \mathbf{c}_k \\
&\qquad + \frac{\partial}{\partial \quad_k^z} \left[S_{+;k}(\mathbf{G})S_{\ ;j}(\mathbf{G}) + S_{\ ;k}(\mathbf{G})S_{+;j}(\mathbf{G}) \right] \mathbf{c}_k^z
\end{aligned}
\tag{65}
$$

where $\mathbf{c}_k^z$ and $\mathbf{c}_k$ are directed unit vectors. The derivative with respect to $\quad_k$ of $S_{\ ;k}(\mathbf{G})$ is:

$$\frac{\partial}{\partial \quad_k}(S_k\ (\mathbf{G})) = e^{i\mathbf{G} \quad \quad_k} e^{\ G\ z_k}(i\mathbf{G}).$$

From which we get:

$$
\begin{aligned}
\frac{\partial}{\partial \quad_k} S &= S_{\ ;j}(\mathbf{G})\frac{\partial}{\partial \quad_k} S_{+;k}(\mathbf{G}) + S_{+;j}(\mathbf{G})\frac{\partial}{\partial \quad_k} S_{\ ;k}(\mathbf{G}) \\
&= (\ i\ _j\ \mathbf{G} \quad \ _j^z\ G)e^{\ i\mathbf{G} \quad \ _j} e^{\ G\ z_j} e^{i\mathbf{G} \quad \quad_k} e^{G\ z_k}(i\mathbf{G}) \\
&\qquad + (\ i\ _j\ \mathbf{G} + \ _j^z\ G)e^{\ i\mathbf{G} \quad \ _j} e^{G\ z_j} e^{i\mathbf{G} \quad \quad_k} e^{\ G\ z_k}(i\mathbf{G}) \\
&= (\ i\ _j\ \mathbf{G} \quad \ _j^z\ G)e^{G\ z_{kj}} + (\ i\ _j\ \mathbf{G} + \ _j^z\ G)e^{G\ z_{jk}}\ (i\mathbf{G})e^{i\mathbf{G} \quad \ _{kj}}
\end{aligned}
\tag{66}
$$

where S, $\ _{kj}$ and z_{kj} are as de ned for the force calculations in *x*5.3.1. Di erentiating $S_{\ ;k}(\mathbf{G})$ with respect to $\ _k^z$ gives:

$$\frac{\partial}{\partial \quad_k^z}(S_k\ (\mathbf{G})) = e^{i\mathbf{G} \quad \quad_k} e^{\ G\ z_k}(\ \ G).$$

So we have

$$
\begin{aligned}
\frac{\partial}{\partial \quad_k^z} S_k &= S_{\ ;j}(\mathbf{G})\frac{\partial}{\partial \quad_k^z} S_{+;k}(\mathbf{G}) + S_{+;j}(\mathbf{G})\frac{\partial}{\partial \quad_k^z} S_{\ ;k}(\mathbf{G}) \\
&= (\ i\ _j\ \mathbf{G} \quad \ _j^z\ G)e^{\ i\mathbf{G} \quad \ _j} e^{\ G\ z_j} e^{i\mathbf{G} \quad \quad_k} e^{G\ z_k} G \\
&\qquad + (\ i\ _j\ \mathbf{G} + \ _j^z\ G)e^{\ i\mathbf{G} \quad \ _j} e^{G\ z_j} e^{i\mathbf{G} \quad \quad_k} e^{\ G\ z_k}(\ \ G) \\
&= (\ i\ _j\ \mathbf{G} \quad \ _j^z\ G)G_z \quad \quad \quad)e^{G\ z_j} e
\end{aligned}
$$

/G [(G)]TJ/F25 7. .

Substituting (66) and (67) into (65) then gives

$$\mathbf{E}_k^{ELC} = \frac{2}{L_x L_y} \sum_{\mathbf{G}\neq 0} \frac{1}{G\,(e^{G\,L_z} - 1)} \sum_{j=1}^{N} \Big(i_j\,\mathbf{G} - {}^{z}_{j}\,G \Big) e^{G\,z_{kj}} + \Big(i_j\,\mathbf{G} + {}^{z}_{j}\,G \Big) e^{G\,z_{jk}}$$
$$(i\mathbf{G})\, e^{i\mathbf{G}\cdot{}_{kj}\,\mathbf{c}_k} + \Big(i_j\,\mathbf{G} - {}^{z}_{j}\,G \Big) G\, e^{G\,z_{kj}} + \Big(i_j\,\mathbf{G} + {}^{z}_{j}\,G \Big)(-G)$$
$$e^{G\,z_{jk}}\, e^{i\mathbf{G}\cdot{}_{kj}\,\mathbf{c}_k} \Big) \hat{\mathbf{z}} \;.$$

Hence, the contribution to the torque from the ELC term is found by taking the cross product of $\mathbf{E}_k^{ELC}$ with ${}_k$ as follows

$${}^{ELC}_{k} = \frac{2}{L_x L_y} \sum_{\mathbf{G}\neq 0} \frac{1}{G\,(e^{G\,L_z} - 1)} \sum_{j=1}^{N} {}_k \Big(i_j\,\mathbf{G} - {}^{z}_{j}\,G \Big) e^{G\,z_{kj}}$$
$$+ \Big(i_j\,\mathbf{G} + {}^{z}_{j}\,G \Big) e^{G\,z_{jk}}\, (i\mathbf{G})\, e^{i\mathbf{G}\cdot{}_{kj}\,\mathbf{c}_k} + {}_k \Big(i_j\,\mathbf{G} - {}^{z}_{j}\,G \Big) G\, e^{G\,z_{kj}}$$
$$+ \Big(i_j\,\mathbf{G} + {}^{z}_{j}\,G \Big)(-G) e^{G\,z_{jk}}\, e^{i\mathbf{G}\cdot{}_{kj}\,\mathbf{c}_k} \Big) \hat{\mathbf{z}} \;.$$

The overall torque is then given by summing the various components discussed in this section:

$${}^{slab}_{k} = {}^{r}_{k} + {}^{slabk}_{k} + {}^{slabsum}_{k} + {}^{ELC}_{k} \;.$$

As mentioned previously the results in this section are a discussion of possibilities only as I was unable to verify the results contained within in the absence of numerical work.

5.4 Errors in Ewald Method for a Con ned Geometry

Clearly, the real space errors are as detailed in *x*3.3 as the real space term (and hence its force and torque have not changed). The reciprocal space errors can also be obtained by taking those derived in the standard geometry and replacing *k* with *G* and K with G. So, neither of these results is recounted here although Brodka[5] observes that the real space error is likely to be overestimated since it takes into account all of the space in the simulation box even though some parts of it are empty of particles.

It is of more interest for us to look at the contribution to the error from the ELC term added to deal with a con ned geometry. This term contributes to the error since it is heavily dependent on the reciprocal space variables *G* and G, which means that the choice of k_c, where k_c is the reciprocal space cut-o as before, will a ect this term. In fact the cut-o in relation to this term is taken to be $G_c = \frac{2\,k_c}{L_x}$ [5].Brodka[5] provides details of the error calculations for U^{ELC} and the results in this section are taken from his work.

As we found for the reciprocal space term in three dimensional geometry there are di erent contributions to the error from the diagonal and o diagonal terms and the overall error contribution is taken to be the sum of these. Using (61) and making substitutions

(as in *x*3.3) by employing a spherical co-ordinate system allows Brodka[5] to state the following:

$$U^{ELC}_{i;off} = \frac{4}{LxLy} \sum_{\mathbf{G}>G_c} \frac{G}{e^{GL_z} - 1} f \sin^2 \quad \cos\, !\,(\ _i; \mathrm{G}) \cos\, !\,(\ _j; \mathrm{G}) \cos(\mathrm{G}\ _{ij}) \cosh(Gz_{ij})$$

$$+ [\sin \quad \cos \quad \cos\, !\,(\ _i; \mathrm{G}) + \sin \quad \cos \quad \cos\, !\,(\ _j; \mathrm{G})] \sin(\mathrm{G}\ _{ij}) \sinh(G\ _{ij})$$

$$\cos^2 \quad \cos(\mathrm{G}\ _{ij}) \cosh(Gz_{ij});$$

$$U^{ELC}_{i;diag} = \frac{2}{LxLy} \sum_{\mathbf{G}>G_c} \frac{G}{e^{GL_z} - 1} [\sin^2 \quad \cos^2\, !\,(\ _i; \mathrm{G}) \quad \cos^2 \ ]:$$

Following this it is again assumed that the positions and orientations are uncorrelated and so the relationships given in (44) can be used to simplify the results above. Making use of the Kronecker delta function and then taking the averages under the assumption of no correlation gives[5]

$$h(\ U^{ELC}_{i;off})^2 i = \frac{^2}{LxLy}\ ^2 \sum_{\mathbf{G}>G_c} \frac{G^2}{(e^{GL_z} - 1)^2} f[\cos^2\, !\,(\ _i; \mathrm{G}) \cos^2\, !\,(\ _j; \mathrm{G}) + 1] h\cosh^2(Gz_{ij}) i$$

$$+ [\cos^2\, !\,(\ _i; \mathrm{G}) + \cos^2\, !\,(\ _j; \mathrm{G})] h\sinh^2(G\ _{ij}) i; \qquad (68)$$

$$h\ \ U^{ELC}_{i;diag} i = \frac{}{LxLy}\ ^2 \sum_{\mathbf{G}>G_c} \frac{G}{e^{GL_z} - 1} [\cos^2\, !\,(\ _i; \mathrm{G}) \quad 1]: \qquad (69)$$

In the continuation of this calculation Brodka[5] rewrites (68) and (69) in integral notation and then evaluates these analytically. Finally he combines the diagonal and o diagonal terms using the following formula for the error of the ELC term in the total potential energy:

$$U^{ELC}_{\ ^2 \ z;} \ ; \ t \frac{1}{2} \sum_{i=1} \sum_{\substack{j=1 \\ j \neq i}} h(\ U^{ELC}_{i;off})^2 i + \sum_{i=1} h\ \ U^{ELC}_{i;diag} i:$$

[Td [(2)11.9552 Tf 21.318 8.087 Td 9.0171

This results in an upper bou.463 8.2 Tf Tf 5.425 337(diplo).996 TE[(6)] 9.4u-409(9.4u-409(t TE[gi0

and h is taken to be the distance between two strips. Care has to be taken not to confuse h with H, which is the height of the strips (i.e. $H = L_z \quad h$).

The method employed by Brodka[5] echoes the method used by Wang and Holm[33] that was recounted in *x*3.3. As was demonstrated in the case of the Ewald method for a standard geometry the same process can be used to perform error calculations relating to the expressions for the force and torque. Once the ideas discussed in *x*5.3 have been developed error calculations and numerical work will test the accuracy of the results obtained. However, due to time restraints this has not been accomplished in this report.

6 Conclusion

This project has provided a comprehensive look at the theory surrounding the Ewald summation and its ability to model dipolar interactions. In any computer simulation the ability to decrease the running times and costs of programs is pivotal and this idea has been discussed throughout this report. The Ewald method itself is computationally effective but this effect can be enhanced by the use of fast Fourier transforms and optimising the parameters. Although this report does not generate new results other than discussions regarding the force and torque contribution from the electrostatic layer correction (ELC) term (as far as I could see such work has yet to be published) it provides a thorough background to the work that has been done previously. The knowledge gained from this provides a spring board to developing the ideas discussed and there is clearly an interest among scientists in furthering this field.

6.1 Further Work

Unfortunately due to the time constraints of this project I was unable to program the formulae discussed in relation to a slab geometry in order to simulate the behaviour here. However, I will continue to work in this area as part of my PhD studies with the aim of publishing any advances made. It will be of great value to use the methods discussed in *x*3.3 and *x*5.4 to perform and verify error calculations for the force and torque contributions from the ELC term in a confined geometry. As part of this I aim to discuss the optimisation of the parameters for dipolar interactions in a confined geometry.

Another obvious action will be to program the results given in *x*5 and once successful to look at the situations this model can be applied to. Its application in the modelling of shear stress in a system of latticed boxes is of particular interest. The Ewald summation cannot be used to model shearing in a system such as that described in *x*2.2 as creating shear between layers of simulation boxes destroys the periodicity inherent in the Ewald method. However, once we can apply the Ewald method to a confined geometry we can use this to our advantage. The walls created to simulate the slab geometry can be used to create the shear, leaving the structure of simulation boxes, and hence the periodicity of the system, unchanged. In initial simulations the top wall can be 'pulled along' at a steady rate to simulate steady shear and later simulations may model more sudden shear by 'pulling' the wall with more force. A further extension to this would be to use a sin function to simulate oscillation of the top wall and model the effect of this on the system. This will have similarities to the work of Wang et al.[34] who modelled shear in electro-rheological (ER) fluids but were unable to implement the Ewald method owing to the restrictions described previously.

Appendix A List of Symbols

Most of the symbols included in this list are given in their general form only although many are used in conjunction with various subscripts and superscripts. The following notes give an idea of the subscripts and superscripts used, although it is not intended to be exhaustive.

Throughout this report a subscript *c* generally means that charge-charge interactions are being discussed whilst a subscript *d* refers to dipole-dipole interactions. If neither subscript is given it is likely to be dealing with dipolar interaction since no subscript is used in chapters dealing with these only. However, be wary as a subscript *c*

N number of particles in the simulation box

q

volume fraction of particles

direction and magnitude of a pair-potential's contribution to error

ω the angle between two vectors

Appendix B Glossary

Brownian motion The presumably random drifting of particles that are suspended in a uid.

charge A unit of matter which is either positive (contains more protons than electrons) or negative (contains more electrons than protons).

colloid A substance dispersed microscopically throughout another substance. In this project we look at magnetic particles dispersed in liquid.

colloidal suspension A material that possesses attributions of more than one state of matter.

complementary error function (denoted by $erfc(x)$) The complement of the Gaussian error function given by $1 \quad erf(x)$.

Coulomb's law A law describing the electrostatic interaction between charged particles. In scalar form it is $\frac{z_i z_j}{4 \quad _0 r^2}$.

coupling constant A measurement of the strength of the force involved in an interaction.

dipole A unit of matter that is negatively charged at one pole and positively charged at the opposite pole.

electro-rheological (ER) uid A uid that changes behaviour when an electrical eld is applied.

electrostatic interaction An interaction between charged particles.

ferro uid A uid with nanometric particles that changes behaviour when a magnetic eld is applied.

free space A perfect vacuum used in theoretical physics to discuss idealised situations.

Gauss error function (denoted by $erf(x)$) A special function used in measurement theory; its use in other areas of maths is not related to errors in measurements except by name.

long range interaction A spatial interaction that decays at a rate no faster than $r^{\ d}$, where r is the molecular separation and d is the dimensionality of the system[1].

magneto-rheological (MR) uid A uid with micrometric particles that changes behaviour when a magnetic eld is applied.

References

[1] M. P. Allen and D. J. Tildesley. *Computer Simulations of Liquids*. Oxford University Press, Oxford, 1987.

[2] Axel Arnold, Jason de Joannis, and Christian Holm. Electrostatics in periodic slab geometries. I. *Journal of Chemical Physics*, 117(6):2496{2502, August 2002.

[3] Ronald N. Bracewell. *The Fourier Transform and Its Applications*. McGraw-Hill Incorporated, London, second edition, 1978.

[4] A. Brodka. Comment on \Electrostatics in periodic slab geometries. I". *Journal of Chemical Physics*, 121(14):7032{7034, October 2004.

[5] A. Brodka. Ewald summation method with electrostatic layer correction for interactions of point dipoles in slab geometry. *Chemical Physics Letters*, 400(1-3):62{67, December 2004.

[6] A. Brodka. Optimal parameter values of the Ewald method with electrostatic layer correction for Coulomb interactions in slab geometry. *Journal of Molecular Structure*, 792-793:56{61, April 2006.

[7] A. Brodka and A. Grzybowski. Electrostatic interactions in computer simulations of a three-dimensional system periodic in two directions: Ewald-type summation. *Molecular Physics*, 117(18):8208{8211, November 2002.

[8] Juan J. Cerda, Ekaterina El mova, V. Ballenegger, Ekaterina Krutikova, Alexey Ivanov, and Christian Holm. Study of the structure factor anisotropy and long range correlations of ferro uids in the dilute low-coupling regime. *Journal of Magnetism and Magnetic Materials*, 323(10):1246{1253, .

[9] Juan J. Cerda, So a Kantorovich, and Christian Holm. Aggregate formation in ferro uid monolayers: Simulations and theory. *Journal of Physics: Condensed Matter*, 20(20):1204125, .

[10] Min-Feng Chung and Chao-Ming Fu. Optical transmittance and dynamic properties of ferro uids (Fe_3O_4) under dc-biased magnetic elds. *IEEE Transactions on Magnetics*, 47(10):3170{3172, October 2011.

[11] S. W. De Leeuw, J. W. Perram, and E. R. Smith. Simulation of electrostatic systems in periodic boundary conditions. I. Lattice sums and dielectric constants. *Proceedings of the Royal Society London A*, 373:57{66, October 1980.

[12] Daan Frenkel and Berend Smit. *Understanding Molecular Simulations: From Algorithms to Application*. Academic Press Limited, London, 1996.

[13] Matteo Frigo and Steven G. Johnson. FFTW, Accessed: August 2012. URL http://www.fftw.org/.

[14] Andrew Gibbs. Molecular dynamics simulation of self-healing polymers. Master's thesis, University of Reading, Reading, March 2011.

[15] A. Grzybowski and A. Brodka. Computationally e cient method for summing interactions of point dipoles in three dimensions with two-dimensional periodicity. *Chemical Physics Letters*, 361(3-4):329{333, July 2002.

[16] Hadi Hezaveh, Alireza Fazlali, and Iman Noshadi. Synthesis, rheological properties and magnetoviscos e ect of Fe_2O_3/ para n ferro uids. *Journal of the Taiwan Institute of Chemical Engineers*, 43(1):159{164, January 2012.

[17] Alan Hinchli e. *Molecular Modelling for Beginners*. John Wiley & Sons Ltd, Chichester, 2003.

[18] William Humphrey, Andrew Dalke, and Klaus Schulten. Vmd: Visual molecular dynamics. *Journal of Molecular Graphics*, 400(1-3):62{67, December 2004.

[19] Alexey O. Ivanov, Zuowei Wang, and Christian Holm. Applying the chain formation model to magnetic properties of aggregated ferro uids.

[25] Modesto T. Lopez-Lopez, Ana Gomez-Ram rez, Laura Rodr guez-Arco, Juan D. G. Duran, Larisa Iskakova, and Andrey Zubarev. Colloids on the frontier of ferro uids. Rheological properties. *Langmuir*, 28(15):6232{6245, March 2012.

[26] M. Mohebi, N. Jamasbi, and Jing Liu. Simulation of the formation of nonequilibrium structures in magnetorheological uids subject to an external magnetic eld. *Physical Review E*, 54(5):5407{5413.

[27] K. W. Morton and D. F. Mayers. *Numerical Solution of Partial Di erential Equations*. Cambridge University Press, Cambridge, 1994.

[28] Nneoma Ogbonna. Molecular dynamics simulation. Master's thesis, African Institute for Mathematical Sciences, Muizenberg, South Africa, May 2004.

[29] William H. Press, Saul A. Teukolsky, William T. Vetterling, and Brian P. Flannery. *Numerical Recipes in C++*. Cambridge University Press, Cambridge, second edition, 2002.

[30] Elena Pyanzina, So a Kantorovich, Juan J. Cerda, and Christian Holm. Structure factor of ferro uids with chain aggregates: Theory and computer simulations. *Journal of Magnetism and Magnetic Materials*, 323(10):1263{1268.

[31] Jason P. Rich, Gareth H. McKinley, and Patrick S. Doyle. Arrested chain growth during magnetic directed particle assembly in yield stress matrix uids. *Langmuir*, 28(8):3683{3689, February 2012.

[32] E. R. Smith and J. W. Perram. Thermodynamic limit for a system with dipole-dipole interactions. *The Journal of the Australian Mathematical Society (Series B)*, 19(1): 116{128, June 1975.

[33] Zuowei Wang and Christian Holm. Estimate of the cuto errors in the Ewald summation for dipolar systems. *Journal of Chemical Physics*, 115(14):6351, October 2001.

[34] Zuowei Wang, Zhifang Lin, and Ruibao Tao. Structure and viscoelasticity of an electrorheological uid in oscillatory shear: Computer simulation investigation. *Journal of Physics D: Applied Physics*, 30(8):1265{1271, April 1997.

[35] Zuowei Wang, Christian Holm, and Hanns Walter Mu ller. Molecular dynamics study on the equilibrium magnetization properties and structure of ferro uids. *Physical Review E*, 66(2):021405, August 2002.

[36] In-Chul Yeh and Max L. Berkowitz. Ewald summation 8(Molecular)-274(d2 11.955d7.776 -17.927